







# Experimental Study of an Optimal Power Management Strategy for Off-Grid RES/Battery System

Y. Aljarhizi\*<sup>‡</sup> , A. Hassoune\*\* , E. Al Ibrahim\* , A. Mesbahi\*\* , M. Khafallah\*\* ,  
A. Nouaiti\*\*\* 

\*Laboratory of Materials Physics and Subatomic, Ibn Tofaïl University, Faculty of Sciences, Kénitra-14000, Morocco.

\*\*Laboratory of Energy & Electrical Systems, ENSEM, Hassan II University of Casablanca-20470, Morocco.

\*\*\* Laboratory of Computer Science, Applied Math and Electrical Engineering, IEVIA team, EST, Moulay Ismail University of Meknes-50040, Morocco.

([aljarhizi.yahya@gmail.com](mailto:aljarhizi.yahya@gmail.com) , [a.hassoune@IEEE.org](mailto:a.hassoune@IEEE.org) , [alibrahmielmehdi@yahoo.fr](mailto:alibrahmielmehdi@yahoo.fr) , [abdelouahed.mesbahi@gmail.com](mailto:abdelouahed.mesbahi@gmail.com) , [m.khafallah@gmail.com](mailto:m.khafallah@gmail.com) , [nouayoub@gmail.com](mailto:nouayoub@gmail.com) )

<sup>‡</sup>Corresponding Author; Y. Aljarhizi, 14000, Tel: +212 648 880 015, [aljarhizi.yahya@gmail.com](mailto:aljarhizi.yahya@gmail.com)

*Received: 11.08.2022 Accepted:23.09.2022*

**Abstract-** This paper presents and analyzes an optimal and an effective power management strategy for a hybrid power system (HPS) intended for off-grid installations. The proposed strategy comprises an optimization algorithm that has been evaluated on a hybrid power system based on a PV/Wind system. In order to improve the power system efficiency, a stationary battery (SB) is used to store the extra energy from renewable energy source (RES). Furthermore, the photovoltaic system is connected to a DC bus through a dc/dc boost converter, while the wind turbine system is connected to the same DC bus via an ac/dc converter linked directly to a single-ended primary inductor converter (SEPIC). However, the proposed management strategy is used to extract as maximum as the power from RES and manage the energy flow via the SB in relation to its state of charge. In order to provide reliable results for this research, a simulation study of two operating modes i.e., RES to Battery (RES2B) and RES to load (RES2L), are realized on MATLAB/Simulink environment. However, the effectiveness of the proposed management strategy is simulated on a 15kW PV system tied to a 10kW wind turbine. The RES power is injected to a 108kWh storage system while the generated power is sensed and distributed to different loads via a 600V DC bus. The obtained results are confirmed and validated by experimental analyzes that are carried out on a laboratory prototype. This experimental test bench had tested the robustness and the efficiency of the proposed management strategy.

**Keywords** Power management strategy, solar energy, wind energy, stationary battery, hybrid power system.

## 1. Introduction

Advanced life quality and inflated mobility sector resulted in higher energy consumption and enormous greenhouse gas emissions. Therefore, the concept of energy-efficient becomes a necessity for every electric infrastructure in order to regulate the electricity flows and increase the quality and dependability of power generation systems. In addition, this concept intends to reduce the imbalances and incompatibilities of electricity generation and its demand, as well as the encouragement of integrating renewable energy sources [1,2].

The integration of renewable energy sources (RES) offers up a new study field of research in which a hybrid power system (HPS) could support the high-power demand while relying less on coal, crude oil, and natural gas as fossil fuels[3]. In the last few years, a number of approaches have been published that demonstrate their efficacy in a multi-sources system comprised of RES and storage batteries [4-9]. In quest of capturing the whole generated power from RES and to overcome the inexistence of the grid power, recent research has been discussed in the literature as reported in [10-14].

Despite the diversity of energy sources, the RES still occasionally suffering from the intermittent nature of climate changes, thus affecting its reliability and efficiency [15]. However, the extensive and fast deployment of RES applications is drawn a lot of attention due to their various advantages. Thus, recent researches have suggested optimization approaches to handle all potential deficiencies, such as using smart power scheduling on the supply system control to support and provide all energy demand according to priority levels [16,17]. To secure the regulated targets from the used HPS, each power source must operate at its maximum potential limit. Therefore, enhanced MPPT algorithms, as discussed in [18,19], are primordial to get hold of the output power of the RES at the highest possible rate.

In the literature, an optimized control strategy and power management are presented in [20] to optimize hybrid WECS/PV/battery and diesel generator micro-grid systems. This technique is used to search for the minimum value of loss of power supply probability. It also keeps a constant DC-bus voltage by controlling the battery operation in order to ensure satisfactory renewable energy factors.

A developed power management strategy as a control unit based on fuzzy logic and PI control is proposed in [21] for a hybrid wind-PV-battery system that is capable of functioning both in on-grid and off-grid modes. While in [22], Particle Swarm Optimization (PSO) is suggested as a management strategy for optimal operation of hybrid PV and wind energy sources with conventional generators in a micro-grid. The comparison between the classic PSO strategy and the PSO power management strategy in [22] concludes that the PSO algorithm has better performance, as shown by a reduction in the final electricity bills and a notable improvement in the production of renewable energy. What distinguishes the power management algorithms used in this work and in [22] is the fact that fewer requirements are needed to apply them experimentally and verify their efficiency compared to other algorithms like the fuzzy logic used in [21]. In addition, a stationary battery (SB) is also used as a backup energy source in order to stabilize the HPS [21,23-26]. This SB is often fitted with a battery management system to monitor in real-time the measurement data e.g., the battery voltage/current and the state of charge (SoC).

The main contribution of this work is to suggest and validate an optimization algorithm for a PV/wind-based hybrid power system intended for off-grid installations. This algorithm can improve the efficiency and the performance of an off-grid power system via two proposed operating modes, i.e., RES2L and RES2B. However, the decision algorithm includes the utilization of stationary batteries in its management strategy. In addition to this contribution in studying and managing hybrid energy systems for solar and wind renewable energies, especially an off-grid system, the novelty of this work is also to show an effective technique of testing and experimental verification of proposed control algorithms by using a laboratory prototype with a reduced power scale prototype based mainly on a TI (Texas Instruments) Solar Explorer Kit and a F28379D DSP. According to that, credible controls in this strategy have been presented and thoroughly analyzed using a simulation study and an experimental evaluation applied on a test bench of a laboratory prototype.

This paper includes Five sections after the introduction; Section 1 describes the proposed hybrid power system and its used controls, while an optimal power management strategy (PMS) is explained in Section 2. Section 3 presents simulation results of the off-grid RES/battery system. Section 4 provides experimental evaluations of the optimal PMS implemented on a reduced power scale prototype. Finally, Section 5 presents the work conclusions.

## 2. Description of the proposed platform

The The Figure 1 illustrates the adopted topology of the off-grid power system and its PMS. The generated power from the RES is injected into the DC bus through two paths of energy flow, i.e., a dc/dc boost converter for photovoltaic array path, and a wind turbine system path through an ac/dc converter directly related to a single-ended primary inductor converter (SEPIC) [27].

Two types of controls in this strategy are suggested and used in this work, such as; the MPPT algorithms for getting the maximum power from solar irradiance and wind speed, and the voltage-current control as another control to avert the overcurrent and the overvoltage of the connected SB.

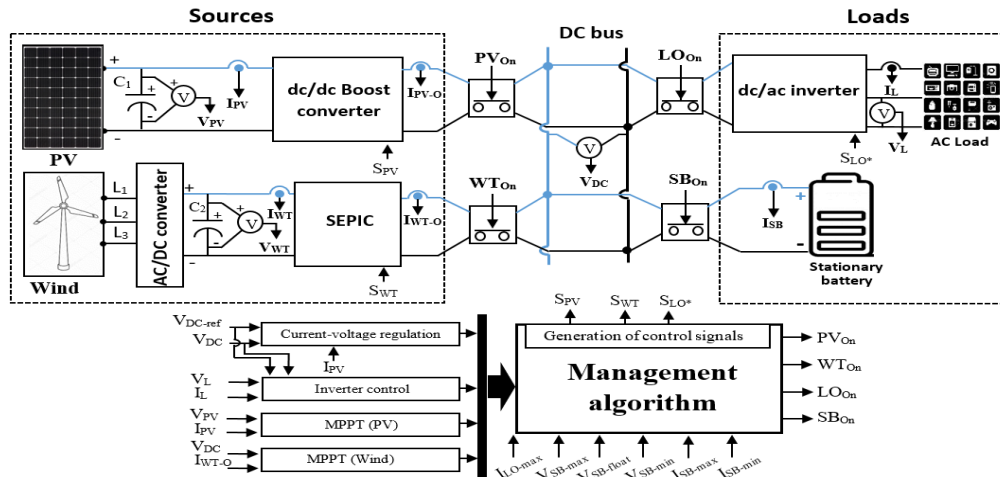


Fig. 1. The proposed management algorithm implemented on a hybrid power system.

### 2.1. Photovoltaic energy conversion system (PECS)

For matching up the specific parameters of the PECS, photovoltaic panels are represented in series/parallel configuration to form a PV array [28,29]. However, the output power of the PV system ( $P_{PV}$ ) is calculated as follows:

$$P_{PV} = V_{PV} \times I_{PV} \tag{1}$$

A unidirectional dc/dc boost converter is used to step up the PV voltage regulated by the MPPT algorithm to the DC bus voltage reference. In addition, the MPPT extracts the maximum power from a solar irradiance profile. The gain of the used boost converter is expressed as:

$$G_S = 1 - \frac{V_{PV}}{V_{DC}} \tag{2}$$

The PV voltage and current are symbolized by  $V_{PV}$  and  $I_{PV}$ , respectively.  $G_S$  symbolizes the variable duty cycle, while the DC bus voltage is represented by  $V_{DC}$ .

In this paper, an incremental conductance (INC) algorithm is suggested to drive the dc/dc boost converter. This algorithm is started by calculating steps, and then measuring the ratio between INC values of PV array power and instantaneous conductance. Then, it will be able to track the MPP, although this requires complicated control circuits and often costly [30,31].

Since the DC bus voltage has to be maintained a constant, the adjustment of the duty cycle that allows for an adaptation of the  $V_{PV}$  to the PV voltage at MPP ( $V_{PV-mpp}$ ) is necessary. Thus, the  $V_{PV}$  is increased by diminishing the  $G_S$  and vice versa. The flowchart of the INC algorithm is given in fig.2.

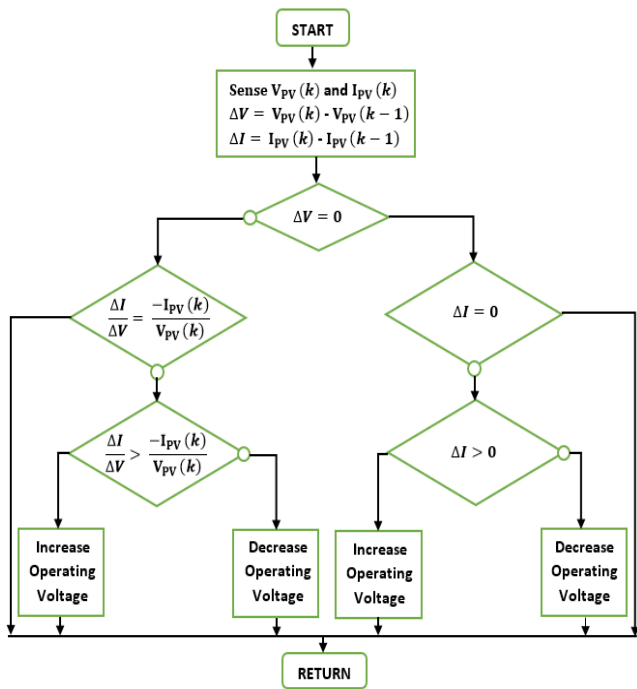


Fig. 2. Flowchart of the INC MPPT algorithm.

### 2.2. Wind Energy Conversion System (WECS)

A wind turbine and a self-excitation induction generator (SEIG) are the main components of the used WECS, their size is depending on the generated power. The association of a 3-phase diode bridge rectifier and a SEPIC [32] is used to adapt the SEIG output voltage to the DC voltage. The proposed block diagram is illustrated in Fig.3.

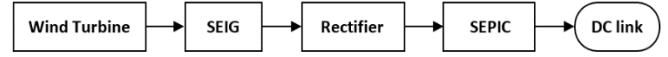


Fig. 3. Block diagram of WECS

#### 2.2.1. Wind Turbine

Aerodynamics illustrates and explains the process of converting wind energy into mechanical energy using wind turbine rotors, which are made up of blades. A wind speed passing via the swept area that is created by rotor blades provokes rotational movement of the whole wind rotors, as a consequence, a mechanical power is produced. The mechanical torque is converted from wind energy by the use of turbine blades, as stated by Eq. (3) [33,34]:

$$C_W = \frac{P_W}{\omega} = \frac{1}{2} \pi \rho R^2 C_p(\lambda, \beta) \frac{V_W^3}{\omega} \tag{3}$$

Where,  $P_W$  symbolizes the wind power that turns the turbine,  $R$  symbolizes the turbine radius (m),  $\rho$  is the air density (usually 1.2251 kg/m<sup>3</sup>),  $V_W$  represents the wind speed in (m/s),  $\lambda$  and  $\beta$  symbolize the tip-speed ratio (TSR) and blade pitch angle, respectively, both of them represented as a function by the power coefficient that symbolized by  $C_p$ . The TSR is calculated as follows:

$$\lambda = \frac{\omega R}{V_W} \tag{4}$$

Where  $\omega$  is the rotor angular speed of the turbine (rad/s). The power coefficient  $C_p$  equation is usually provided by the turbine manufacturer as a polynomial transfer function reflecting obtainable electrical power versus wind speed. To model  $C_p(\lambda, \beta)$ , a generic equation is used as follows [35,36]:

$$C_p(\lambda, \beta) = 0.576 \left( \frac{116}{\lambda_i} - 0.4\beta - 5 \right) \exp \frac{21}{\lambda_i} + 0.0068\lambda \tag{5}$$

With,

$$\lambda_i = \frac{1}{\lambda_i + 0.08\beta} - \frac{0.035}{\beta^3 + 1} \tag{6}$$

The power coefficient is required to be maintained at its maximum for enabling the wind generator source to produce maximum power at the optimum TSR. As indicated in [33], the maximum of power coefficient ( $C_{Pmax}=0.48$ ) is achieved at  $\lambda_{opt}=8.1$ . However, the optimum torque and the maximum power are presented in Eq. (7) and (8).

$$C_{W-opt} = K \omega_{opt}^2 \tag{7}$$

$$P_{W-max} = K \omega_{opt}^3 \tag{8}$$

Where  $K$  is the curve gain of the optimum torque, expressed by:

$$K = \frac{1}{2} \pi \rho C_{Pmax} \frac{R^5}{\lambda_{opt}^3} \quad (9)$$

From Eq. (8), the maximum power is achieved by adjusting the shaft speed for different wind speed values, following the MPPT algorithm, that controls the WECS. The pitch angle of the wind turbine is fixed to zero, so that the mechanical output power of the turbine PM will be expressed as:

$$P_M = C_P(\lambda) P_W \quad (10)$$

### 2.2.2. Single Ended Primary Inductor Converter (SEPIC)

This type of dc/dc converters is called SEPIC, it can provide an output voltage equal to its input voltage, also higher or less. The SEPIC scheme involves a buck-boost converter preceded by a boost converter [37]. The output voltage of the SEPIC is adjusted to the DC bus voltage by controlling the power transistor, such a case is utilized in conventional buck-boost converter. This converter is similar, except the special feature and main advantage of SEPIC, that provides the same voltage polarity of its output and input [38].

The SEPIC system is shown in Fig. 4. The output voltage rises when the switch  $S_1$  is turned on and it drops when  $S_1$  is turned off. The ripple voltage and voltage loss across the diode  $D_1$  terminal are ignored in the steady-state mode.

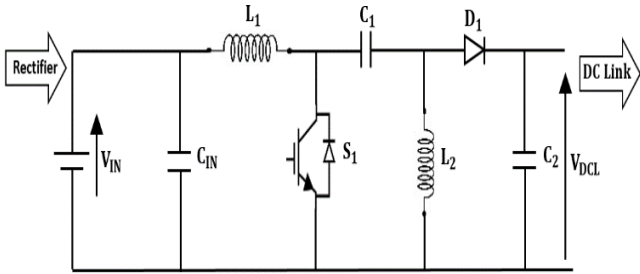


Fig. 4. scheme of SEPIC.

During the  $S_1$  on-time, the voltage rate of  $L_1$  and  $L_2$  can be expressed as:

$$V_{L1} = V_{IN} \quad (11)$$

$$V_{L2} = V_{C1} \quad (12)$$

During the  $S_1$  off-time, the voltage between  $L_1$  and  $L_2$  is described as follows:

$$V_{L1} = V_{IN} - V_{C1} - V_{DCL} \quad (13)$$

$$V_{L2} = -V_{DCL} \quad (14)$$

Eq. (15) and Eq. (16) present the volt-second expressions of  $L_1$  and  $L_2$ , respectively.

$$V_{IN} D_s T_s + (V_{IN} - V_{C1} - V_{DCL})(1 - D_s) T_s = 0 \quad (15)$$

$$V_{C1} D_s T_s - V_{DCL}(1 - D_s) T_s = 0 \quad (16)$$

Where,  $D_s$  is the duty cycle of  $S_1$ .

$$D_s = \frac{t_1 - t_0}{T_s} \quad (17)$$

From Eq. (15) and (16), the ratio between  $V_{DCL}$  and  $V_{IN}$  can be defined as follows:

$$V_{DCL} = V_{IN} \frac{D_s}{1 - D_s} \quad (18)$$

### 2.3. DC bus power

The DC bus is the main key element of the proposed controls, in which real-time processing is necessary to validate the proposed PMS [39]. A typical PV/Wind system generates the power flow, that is occasionally supported by SB in order to match the user requirements in terms of energy demand [40].

The representation of the DC bus scheme is shown in Fig. 5. It composed by two renewable sources gathered in the upstream section. Besides, the AC load and the SB are reassembled in the downstream block.

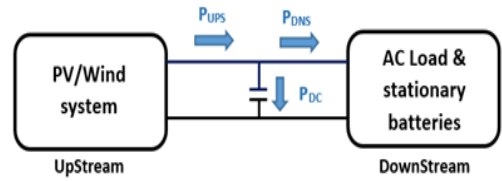


Fig. 5. DC bus power flow.

Equation (19) regroups the two forms of blocks.

$$P_{DC} = P_{UPS} - P_{DNS} \quad (19)$$

Where  $P_{UPS}$  represents the total power generated by the upstream block,  $P_{DNS}$  represents the power at the SB and the AC load, while  $P_{DC}$  represents the DC bus power.

The Eq. (20) as a deriving function of DC bus voltage ( $V_{DC}$ ) is used to calculate the DC bus power, where a coupling capacitor ( $C$ ) distinct the DC bus.

$$P_{DC} = C V_{DC} \frac{dV_{DC}}{dt} \quad (20)$$

The DC power is influenced by the variations of solar irradiation for the PECS, the wind speed for the WECS, and the SoC for the SB. Also, the power demand from AC load ( $P_{ACL}$ ). The power flow between all sources and loads is represented in Eq. (21).

$$P_{DC} = P_{PV} + P_{WT} \pm P_{SB} - P_{ACL} \quad (21)$$

## 3. Optimal power management algorithm (PMA)

The power management algorithm (PMA) is comprised of two operating modes i.e. RES2B and RES2L. These two modes are proposed and analyzed in order to increase the efficiency of the HPS. However, the flowchart of the proposed PMA is shown in Fig. 6.

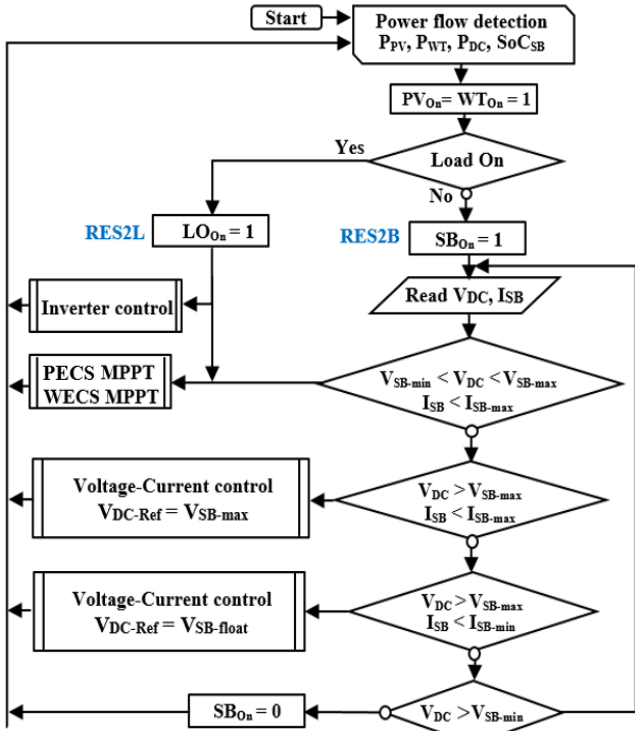


Fig. 6. Flowchart of the optimal power management algorithm (PMA).

The load On state is a principal element to determine which operating mode must be set in order to meet the user requirements and to achieve a high level of independency for the overall installation.

3.1. Mode 1: RES2B

In RES2B mode, three power switches are activated i.e., PV<sub>On</sub>, WT<sub>On</sub>, and SB<sub>On</sub>. The PMS explores the advantages of its algorithm, for benefiting from the period of MPPT mode to the fullest extent, plus the rapid switching to voltage-current control, reciprocally. In this regard, the SB is charged via three different phases as illustrated in Fig. 7.

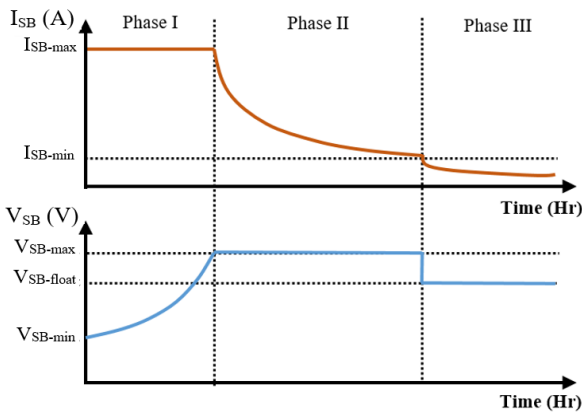


Fig. 7. SB charging phases.

In Phase I, the charging operating is started by adopting MPPT algorithms for both converters, the dc/dc boost converter and the SEPIC as long as the charging voltage of the SB is between its minimum value ( $V_{SB-min}$ ) and its maximum

value ( $V_{SB-max}$ ). In the meantime, the charging current ( $I_{SB}$ ) is set to its maximum value ( $I_{SB-max}$ ).

Once  $V_{SB}$  attained  $V_{SB-max}$ , the converters are now running at overcharge phase which is the second phase. The charging current is maintained decreasing until it drops below  $I_{SB-min}$  (Phase III), indicating that the float charge phase has been reached, at this point, the reference voltage will be readjusted to a reduced value ( $V_{SB-float}$ ) by the PMA. This decrease, which generates a small charging current, will avoid the battery from an eventual deep self-discharge [41].

3.2. Mode 2: RES2L

In this mode, the RES delivers their maximum power to the AC load while the management system controls three power switches, i.e., PV<sub>On</sub>, WT<sub>On</sub> and LO<sub>On</sub>. Meanwhile, the control strategy set by the PMA will fine-tune the MPPT algorithms to drive both the boost converter and SEPIC, and then control the dc/ac converter.

4. Simulation results

To assess the proposed PMS, a hybrid power system has been designed and modelled on Matlab/Simulink in order to simulate the two operating modes i.e., Mode 1 (RES2B): SB charging mode from solar panels through a boost converter, and from wind turbine via a SEPIC converter, and Mode 2 (RES2L) as utilization mode: for injecting power into the AC load from RES by using a dc/dc boost converter and SEPIC, both followed by a dc/ac inverter.

The modelled system comprises a PV system of 15kW, and a wind turbine system of 10kW. The voltage of the DC bus is chosen to be 600V. In addition, a 108kWh storage system is set to represent the SB. Fig. 8 illustrates the modelled system and its monitoring system in Matlab/Simulink.

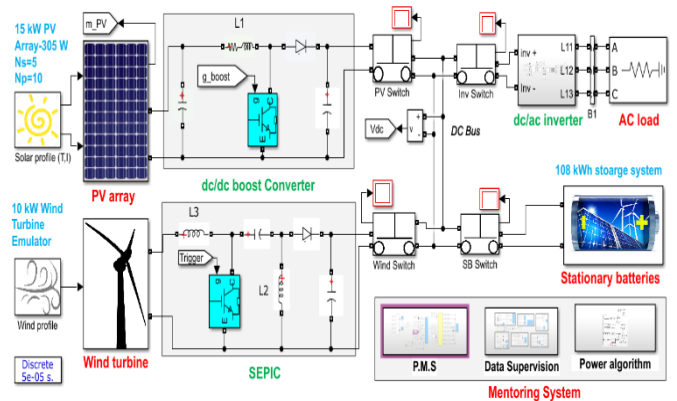
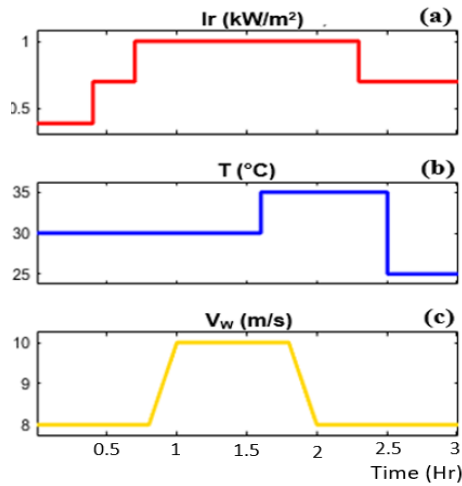


Fig. 8. Topology of the proposed power system in Matlab/Simulink.

In order to test the validity of the advanced PMA, the simulation study proposes a climatic scenario for the AC load. Therefore, the aim is to fulfill the AC load power demand by activating mode 2. In this case, the load would be given high priority to link up to RES. Fig.9 presents the proposed climatic scenario timeline of solar irradiation, temperature and wind speed.

C



**Fig. 9.** The proposed scenarios versus time (a) Irradiance; (b) Temperature; (c) Wind speed.

4.1. Mode 1: RES2B

Figure 10 shows the evolution of the charging power of SB as regards a change in temperature, irradiation, and wind speed versus time, where three power switches are activated i.e. PV<sub>On</sub>, WT<sub>On</sub> and SB<sub>On</sub>.

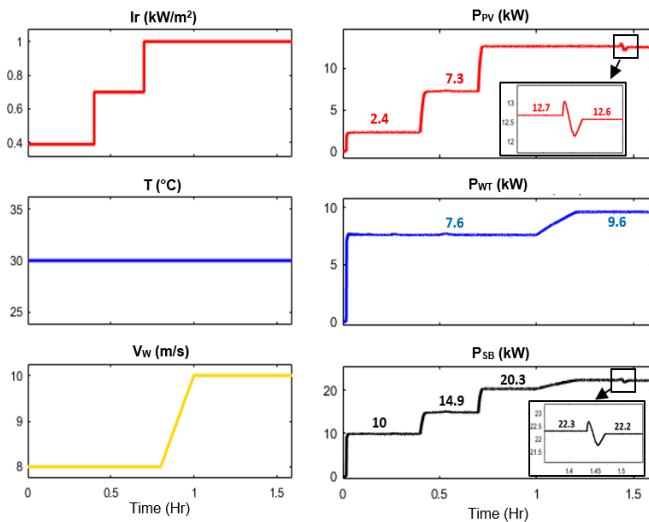


**Fig. 10.** Power curves in mode 1 versus time.

At the start of the simulation, the system aims to extract the maximum power from PV/Wind system based on the MPPT algorithms, as long as the charging voltage does not exceed the maximum charging value. Under these conditions, the off-grid power system attains better energy efficiency, wherein the losses of energy are only associated with the components of the power converters. After  $t = 0.4$ h, the irradiance is increased to  $0.7 \text{ kW/m}^2$ , consequently, the PV power is increased to  $7.3 \text{ kW}$ , and the same variation is manifested at  $t = 0.7$ h. Therefore, the temperature has a reverse impact on PV energy than irradiation, that is to say, when the temperature increases, the power decreases slightly.

The wind system starts to operate at a wind speed equal to  $8 \text{ m/s}$ , this rate allows the WECS to capture a wind power equal to  $7.6 \text{ kW}$ . Once the wind speed reaches  $10 \text{ m/s}$ , the wind power increases up to  $9.6 \text{ kW}$ . Therefore, the charging rate of power follows the variation of wind speed throughout the simulation time. Fig.11 shows the charging current and the SoC of the SB.

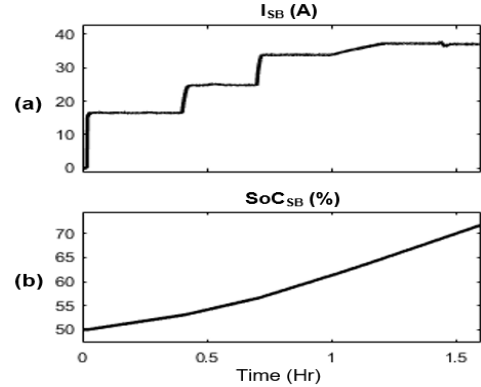


**Fig. 11.** Charging process in mode 1 versus time (a) Current; (b) SoC.

As it can be seen in Fig.11, the variation of wind speed and irradiance has an impact on the slope of the SoC curve which is characterized by its increasing tilt rate. The PMA simulation result is shown in Fig.12.

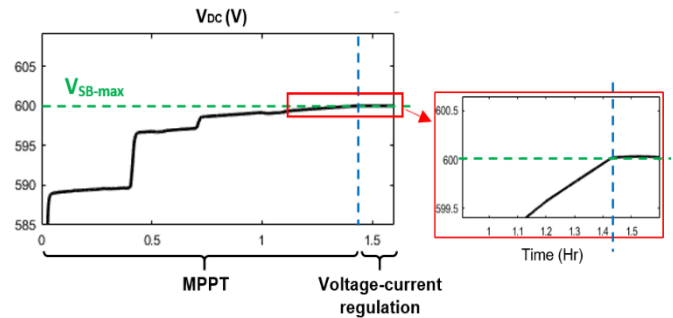


**Fig. 12.** Charging voltage in mode 1 versus time.

At the beginning, the dc/dc boost converter and the SEPIC were controlled by MPPT algorithms until the charging voltage reached  $V_{SB-max}$  at  $t = 1.45 \text{ Hr}$ , then the PMA switched the control to voltage-current regulation. However, it is noticed from the obtained results that the adopted system does not present any problem of voltage imbalance at the DC bus. Also, the proposed control strategy shows a rapid dynamic response in the event of a quick change in solar irradiation and in wind speed.

4.2. Mode 2: RES2L

In this mode, the boost converter and the SEPIC are both controlled by MPPT algorithms on a full-time basis. The simulation results of RES2L mode are presented in the Figs. 13-15.

C

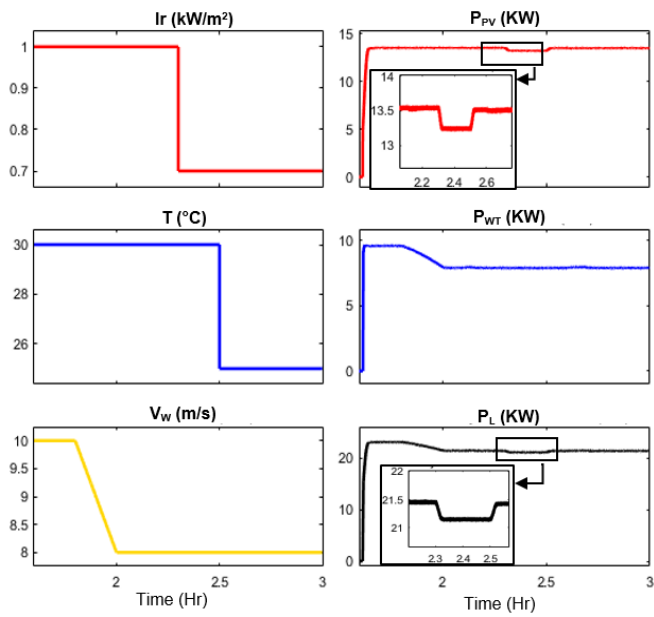


Fig. 1. Power curves in mode 2 versus time.

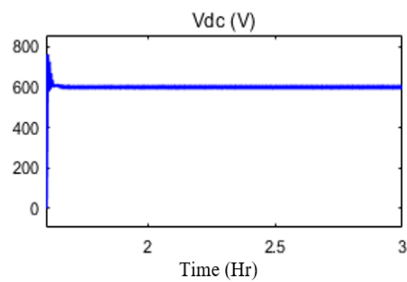


Fig. 2. DC bus voltage in mode 2 versus time.

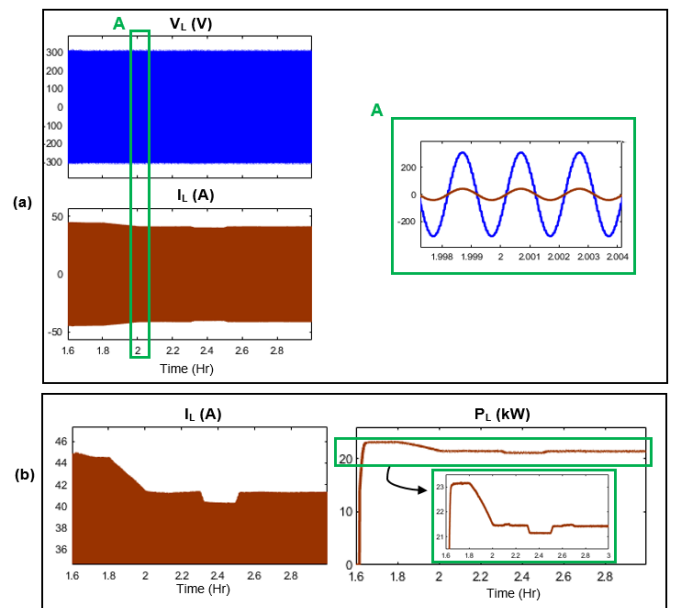


Fig. 3. Voltage and current curves of AC load in mode 2 versus time.

The DC bus voltage is maintained at 600V due to the control of the dc/ac inverter. The fluctuations at the transient state are minimized with a high level of efficiency.

## 5. Experimental evaluation

The efficiency of the proposed strategy's controls is tested by using a laboratory prototype that represents the off-grid HPS. The experimental setup is shown in Figs.16-a, b where the proposed PMA will be validated. The platform includes a TI (Texas Instruments) Solar Explorer Kit, a F28379D DSP, Hall effect sensors and batteries.

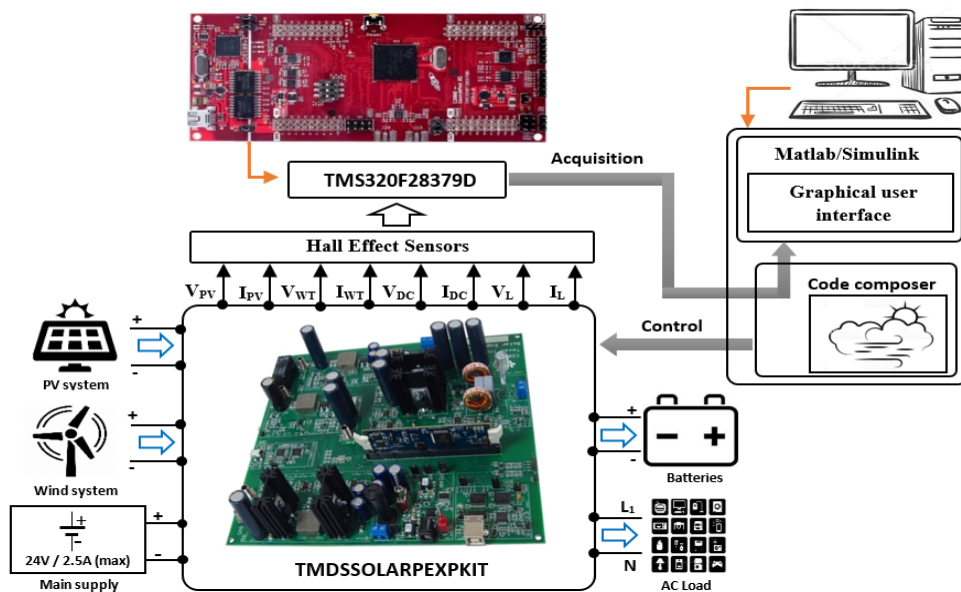
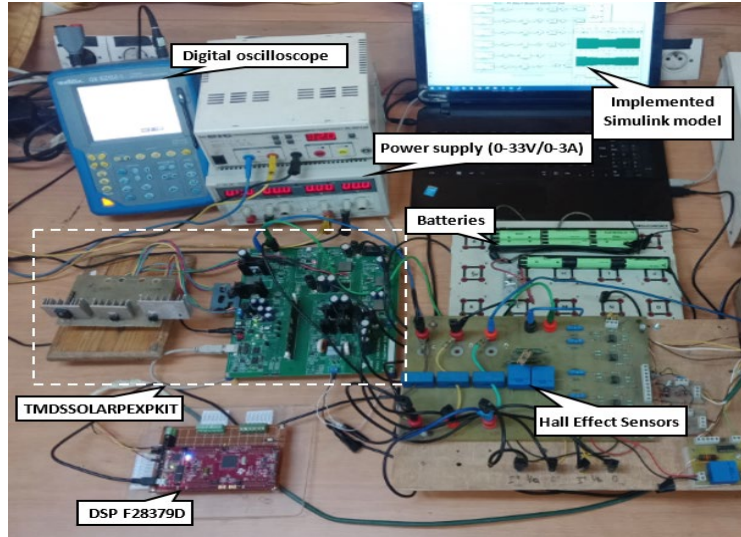


Fig. 16-a. Schematic of the proposed test bench



**Fig. 16-b.** Experimental setup

To emulate the HPS, a TI board with an integrated buck-boost stage is used, and a 12V-4000mAh battery is utilized in place of the SB. Multiple operating modes can be simulated just by varying the irradiation value or wind speed. Since this is a scaled-down version, the RES output voltages are limited to 18.46V, while the rate of  $I_{L-max}$  is limited to 4A.

The emulated power system is controlled by two internal DSPs. The real time monitoring process is done with a F28379D DSP tied to the IT board through an external mode in Simulink. Regarding to steady-state performance and transient-performance, experimental tests were performed over a 10 minutes of time period. The Figs.17-22 show the experimental results of the two proposed operating modes.

*5.1. Experimental results for mode 1*

In this mode, the implemented buck-boost stage emulates the DC voltage of the wind turbine at the ac/dc converter output as represented in Fig.1. This DC voltage ( $V_{WT-DC}$ ) is changed based on the wind speed as illustrated in Fig.17

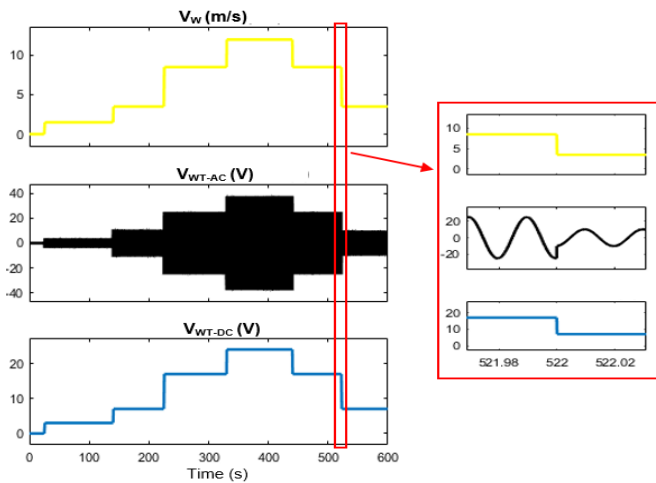


**Fig. 17.** Experimental outputs describing the AC and the DC wind turbine voltage versus wind speed in mode 1.

Figs.18-20 show the results obtained when the Lithium-ion batteries are charging through two different modes of

regulation. Note that the voltage  $V_{DC}$  is the charging voltage of the connected batteries.

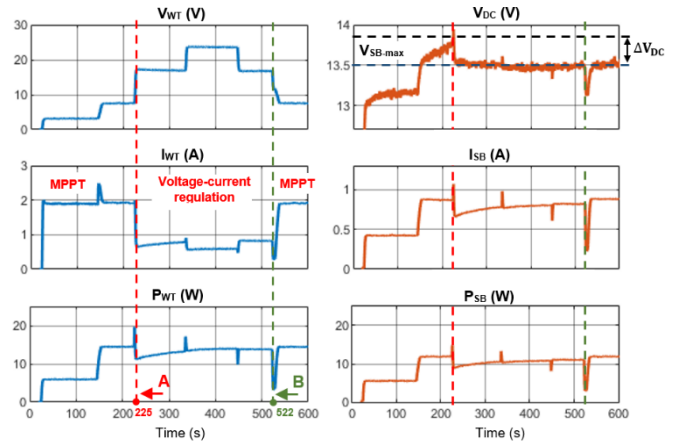


**Fig. 18.** Experimental outputs of the of SB charging process in mode 1.

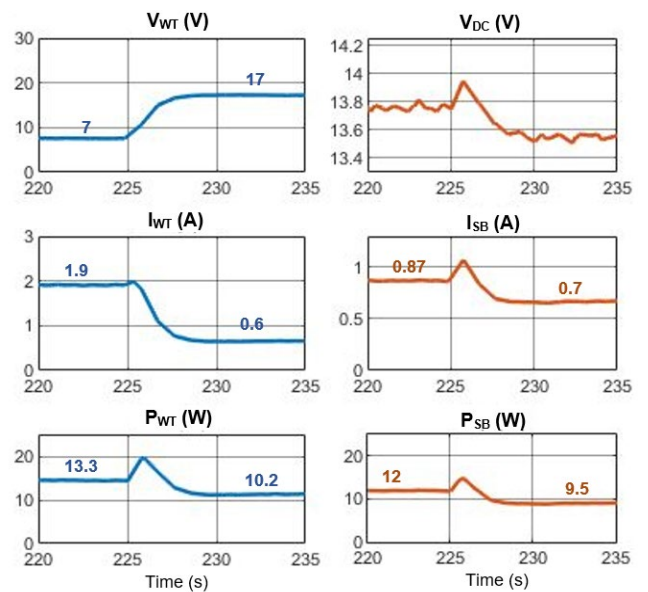


**Fig. 19.** Experimental outputs of switching from MPPT control to voltage-current control.



At first, the system has extracted the maximum of the available wind power while controlling the SEPIC using the MPPT algorithm. After  $t = 225s$ , the  $V_{DC}$  voltage has exceeded the maximum value of the charging voltage ( $V_{SB-max} = 13.5V$ ). Therefore, the SEPIC control strategy is switched to voltage-current control in order to prevent damage to the batteries and to avoid any overcharging in terms of voltage.

Following the change in wind speed, Fig.20 illustrates the control strategy transition from voltage-current into MPPT. At  $t = 522s$ ,  $V_{WT-DC}$  decreases to 7V, this voltage rate matches the  $V_{DC}$  rate that is lower than that of  $V_{SB-max}$ .

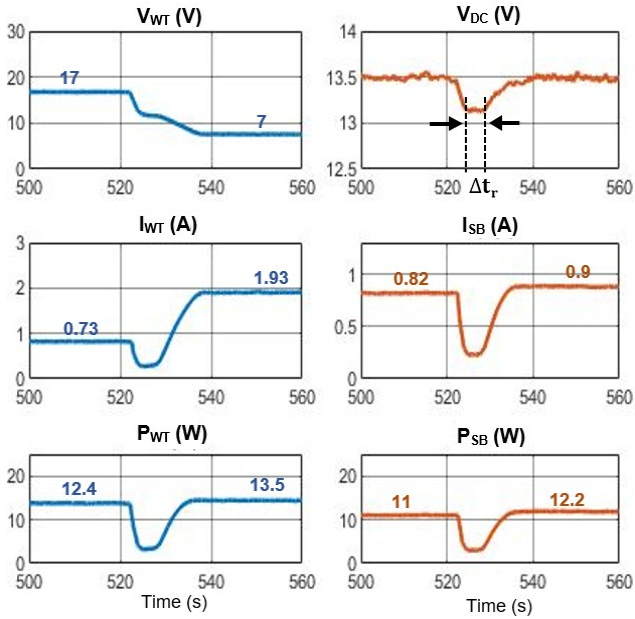


**Fig. 20.** Experimental outputs of switching from voltage-current control mode into MPPT mode.

Control under MPPT algorithm has resulted an increase in charging power up to 12.2W. The control system has a response time ( $\Delta t_r$ ) that is required to process the current and the voltage measurements in real time and act on them to apply the appropriate control in the strategy. Based on these experimental results, the wind turbine system delivers an average efficiency of more than 90%, it also presents an improved performance which can be explained by the quick pursuit from the outputs of the proposed optimal PMA.

5.2. Experimental results for mode 2

One of the main objectives of this work is to ensure low voltage changes over the range of specified values for steady state voltage at DC bus, we therefore use the MPPT algorithm for dc/dc boost converter. In this mode, a unipolar modulation technique is used to generate the control pulses, this technique consists of a single rectified sinusoidal reference signal, which is compared to a high frequency triangular carrier. However, the output voltage and current of the dc/dc boost converter ( $V_{DC}$ ,  $I_{DC}$ ), are shown in Fig.21, as well as the obtained voltage and current from the PV panels emulator ( $V_{PV}$ ,  $I_{PV}$ ).

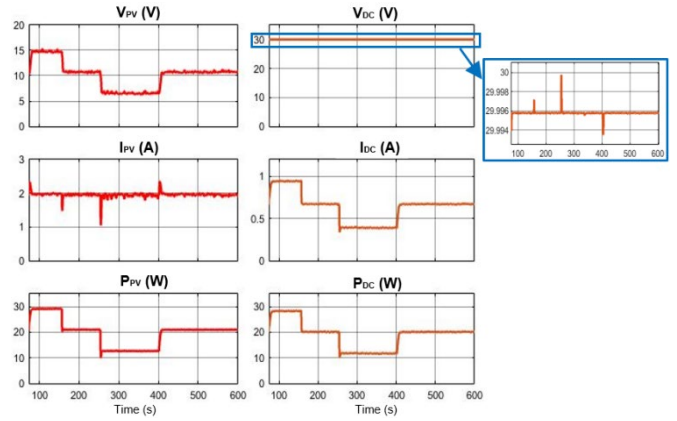


**Fig. 21.** Experimental outputs describing the dc/dc boost converter controlled by MPPT algorithm in mode 2.

The experimental results in Fig.22 and 23 correspond to the AC load voltage ( $V_L$ ) and current ( $I_L$ ). Considering the AC load as resistive load, it is noted that the power factor rate has been well respected with a better tracking of the reference.

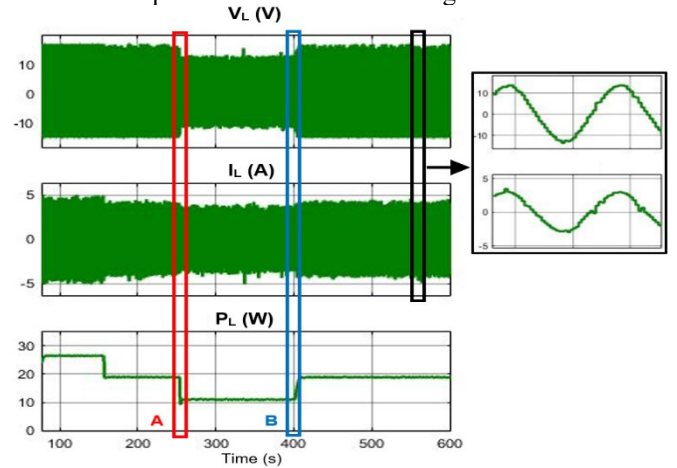


**Fig. 22.** Experimental outputs describing the dc/ac inverter in mode 2.

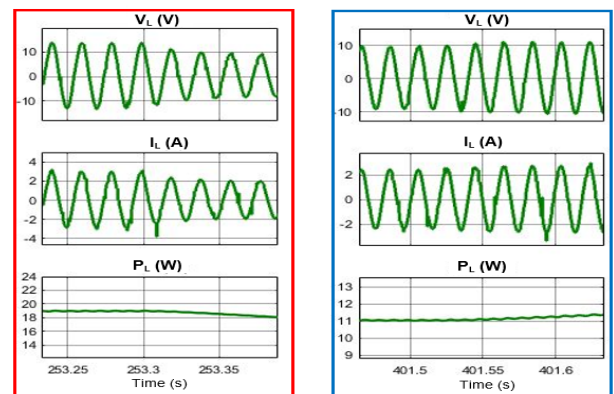


**Fig. 23.** Experimental outputs describing the variation of AC power in mode 2 (Zoom A & B in Fig. 22).

As it can be seen from the presented results, the PMA allows the HPS to react quickly and efficiently whatever the type of the selected load (SB or AC load). In this part of the study, the experimental results have proven the validity of the simulation results via a reduced power scale prototype emulating a multi-source system.

## 6. Conclusion

In this paper, an improved topology of a hybrid power system is presented in detail to analyze an optimal power management strategy. For achieving a high level of efficiency for the power system in terms of voltage profile maintaining and power loss minimization, the proposed power management algorithm was tested on various case scenarios to emulate two operating modes i.e., RES2B, RES2L.

The operating modes had been validated by simulation results carried out in Matlab/Simulink software and by experimental evaluations using a reduced power scale prototype. The adopted energy optimization approach had proven gainful outcomes from maximizing the RES output power by using MPPT algorithms, and it would maintain a smooth integration of other RES. In addition, the proposed algorithm had prevented damage to the stationary batteries from overvoltage state and from self-deep discharge. In future work, the PMS in this research will be developed by including other operating modes and comparing them experimentally in order to further enhance the performance of the HPS-based RES.

## References

- [1] E. I. Come Zebra, H. J. van der Windt, G. Nhumaio, and A. P. C. Faaij, "A review of hybrid renewable energy systems in mini-grids for off-grid electrification in developing countries," *Renewable and Sustainable Energy Reviews*, vol. 144, p. 111036, Jul. 2021.
- [2] O. Babatunde, J. Munda and Y. Hamam, "Off-grid hybrid photovoltaic – micro wind turbine renewable energy system with hydrogen and battery storage: Effects of sun tracking technologies", *Energy Conversion and Management*, vol. 255, p. 115335, Mar. 2022.
- [3] I. M. Opedare, T. M. Adekoya and A. Longe, "Optimal Sizing of Hybrid Renewable Energy System for off-Grid Electrification: A Case Study of University of Ibadan Abdusalam Abubakar Post Graduate Hall of Residence", *International Journal of Smart grid*, 2020.
- [4] Z. Dostál and L. Ladányi, "Demands on energy storage for renewable power sources," *Journal of Energy Storage*, vol. 18, pp. 250–255, Aug. 2018.
- [5] I. A. Nassar, K. Hossam, and M. M. Abdella, "Economic and environmental benefits of increasing the renewable energy sources in the power system," *Energy Reports*, vol. 5, pp. 1082–1088, Nov. 2019.
- [6] S. B. Wali, M. A. Hannan, M. S. Reza, P. J. Ker, R. A. Begum, M.S. Abd Rahman, and M. Mansor, "Battery storage systems integrated renewable energy sources: A bibliometric analysis towards future directions", *Journal of Energy Storage*, vol. 35, p. 102296, Mar.2021.
- [7] J. Xie, Z. Li, Y. Xia, L. Liang, and W. Zhang, "Optimizing capacity investment on renewable energy source supply chain," *Computers & Industrial Engineering*, vol. 107, pp. 57–73, May 2017.
- [8] H. Bamdjid, M. Benhami, A. Harrouz, R. Abbas, I. Colak, F. Bouazza, V. Dumbrava, and K. Kayisli, "Photovoltaic/Wind Hybrid System Power Stations to Produce Electricity in Adrar Region," 2022 10th International Conference on Smart Grid (icSmartGrid), Jun. 2022.
- [9] A. A. Ameri, M. B. Camara, and B. Dakyo, "Efficient Energy Management for Wind-Battery Hybrid System Based Variable Frequency Approach," 2021 10th International Conference on Renewable Energy Research and Application (ICRERA), Sep. 2021.
- [10] B. Park and J. Hur, "Spatial prediction of renewable energy resources for reinforcing and expanding power grids," *Energy*, vol. 164, pp. 757–772, Dec. 2018.
- [11] O. E. Olabode, T. O. Ajewole, I. K. Okakwu, A. S. Alayande, and D. O. Akinyele, "Hybrid power systems for off-grid locations: A comprehensive review of design technologies, applications and future trends," *Scientific African*, vol. 13, p. e00884, Sep. 2021.
- [12] M. Dib, M. Ramzi, and A. Nejmi, "Voltage regulation in the medium voltage distribution grid in the presence of renewable energy sources," *Materials Today: Proceedings*, vol. 13, pp. 739–745, 2019.
- [13] A. Saïdi, A. Harrouz, I. Colak, K. Kayisli, and R. Bayindir, "Performance Enhancement of Hybrid Solar PV-Wind System Based on Fuzzy Power Management Strategy: A Case Study," 2019 7th International Conference on Smart Grid (icSmartGrid), Dec. 2019.
- [14] N. Altin and S. E. Eyimaya, "A Review of Microgrid Control Strategies," 2021 10th International Conference on Renewable Energy Research and Application (ICRERA), Sep. 2021.
- [15] F. Javed, "Impact of Temperature & Illumination for Improvement in Photovoltaic System Efficiency", *International Journal of Smart grid*, no. 61, 2022.
- [16] H. Chamandoust, G. Derakhshan, S. M. Hakimi, and S. Bahramara, "Tri-objective scheduling of residential smart electrical distribution grids with optimal joint of responsive loads with renewable energy sources," *Journal of Energy Storage*, vol. 27, p. 101112, Feb. 2020.
- [17] A. Hassoune, M. Khafallah, A. Mesbahi, L. Benaouinate, and T. Bouragba, "Control Strategies of a Smart Topology of EVs Charging Station Based Grid Tied RES-Battery," *International Review of Electrical Engineering (IREE)*, 13(5), 385-396, 2018.
- [18] O. Zebraoui and M. Bouzi, "Improved MPPT controls for a standalone PV/wind/battery hybrid energy system," *International Journal of Power Electronics and Drive Systems (IJPEDS)*, vol. 11, no. 2, p. 988, Jun. 2020.
- [19] Y. Aljarhizi, A. Hassoune, and E. Al Ibrahim, "Control Management System of a Lithium-ion Battery Charger Based MPPT algorithm and Voltage Control," 2019 5th International Conference on Optimization and Applications (ICOA), Apr. 2019.

- [20] J. Bandopadhyay and P. K. Roy, "Application of hybrid multi-objective moth flame optimization technique for optimal performance of hybrid micro-grid system," *Applied Soft Computing*, vol. 95, p. 106487, Oct. 2020.
- [21] K. Basaran, N. S. Cetin, and S. Borekci, "Energy management for on-grid and off-grid wind/PV and battery hybrid systems," *IET Renewable Power Generation*, vol. 11, no. 5, pp. 642–649, Feb. 2017, doi: 10.1049/iet-rpg.2016.0545.
- [22] A. Kerboua, F. Boukli-Hacene, and K. A. Mourad, "Particle Swarm Optimization for Micro-Grid Power Management and Load Scheduling," *International Journal of Energy Economics and Policy*, vol. 10, no. 2, pp. 71–80, Jan. 2020.
- [23] P. Gajewski and K. Pieńkowski, "Control of the Hybrid Renewable Energy System with Wind Turbine, Photovoltaic Panels and Battery Energy Storage", *Energies*, vol. 14, no. 6, p. 1595, 2021.
- [24] A. Colak and K. Ahmed, "A Brief Review on Capacity Sizing, Control and Energy Management in Hybrid Renewable Energy Systems," 2021 10th International Conference on Renewable Energy Research and Application (ICRERA), Sep. 2021.
- [25] L. Barote and C. Marinescu, "Li-Ion energy storage capacity estimation in residential applications with EV," 2019 8th International Conference on Renewable Energy Research and Applications (ICRERA), Nov. 2019.
- [26] Y. M. Mendi, M. Demirtas, and H. E. Akinc, "Importance of Lithium-Ion Energy Storage Systems in Balancing the Grid: Case Study in Turkey," 2021 10th International Conference on Renewable Energy Research and Application (ICRERA), Sep. 2021.
- [27] A. Hassoune, M. Khafallah, A. Mesbahi, and T. Bouragba, "An Improved Approach of Control for a Battery Charger Based Forward Converter and SEPIC," 2018 6th International Renewable and Sustainable Energy Conference (IRSEC), Dec. 2018.
- [28] C. Saiprakash, A. Mohapatra, B. Nayak, and S. R. Ghatak, "Analysis of partial shading effect on energy output of different solar PV array configurations," *Materials Today: Proceedings*, vol. 39, pp. 1905–1909, 2021.
- [29] A. Nouaiti, A. Saad, A. Mesbahi and M. Khafallah, "A new efficient topology of single-phase five-level inverter for PV system." *International Journal of Engineering and Technology Innovation* 8.4 (2018): 241.
- [30] D. Ounnas, D. Guiza, Y. Soufi and M. Maamri, "Design and Hardware Implementation of Modified Incremental Conductance Algorithm for Photovoltaic System", *Advances in Electrical and Electronic Engineering*, vol. 19, no. 2, Jul. 2021.
- [31] A. Belkaid, I. Colak, K. Kayisli and R. Bayindir, "Design and Implementation of a Cuk Converter Controlled by a Direct Duty Cycle INC-MPPT in PV Battery System", *International Journal of Smart grid*, 2019.
- [32] J. Hussain and M. K. Mishra, "Design of current mode controlled SEPIC DC-DC converter for MPPT control of wind energy conversion systems," 2015 International Conference on Computation of Power, Energy, Information and Communication (ICCPEIC), Apr. 2015.
- [33] L. Benaouinate, M. Khafallah, A. Mesbahi, A. Martinez, Development of a useful Wind Turbine Emulator Based on Permanent Magnet DC Motor, 14th International Multi-Conference on Systems, Signals & Devices, March, 2017, Marrakech, Morocco.
- [34] Y. Aljarhizi, E. Al Ibrahim, A. Mesbahi, A. Hassoune, and M. Khafallah, "Static Power Converters for a Wind Turbine Emulator Driving a Self-Excited Induction Generator," 2020 1st International Conference on Innovative Research in Applied Science, Engineering and Technology (IRASET), Apr. 2020.
- [35] A. Mesbahi, Y. Aljarhizi, A. Hassoune, M. Khafallah, and E. Al Ibrahim, "Boost Converter implementation for Wind Generation System based on a variable speed PMSG," 2020 1st International Conference on Innovative Research in Applied Science, Engineering and Technology (IRASET), Apr. 2020.
- [36] S. Benzaouia, M. Mokhtari, S. Zouggar, A. Rabhi, M. L. Elhafyani, and T. Ouchbel, "Design and implementation details of a low cost sensorless emulator for variable speed wind turbines," *Sustainable Energy, Grids and Networks*, vol. 26, p. 100431, Jun. 2021.
- [37] S. Venkatanarayanan, M. R. M. Nanthini, Design and Implementation of SEPIC and Boost Converters for Wind and Fuel cell Applications, *International Journal of Innovative Research in Science, Engineering and Technology*, vol. 3 no. 3, March 2014, pp. 378-383.
- [38] I. Ahmed and T. Kahawish, "Design and Implementation of High Gain SEPIC Converter," 2021 International Conference on Advanced Computer Applications (ACA), Jul. 2021.
- [39] C. Albea-Sánchez, "Hybrid dynamical control based on consensus algorithms for current sharing in DC-bus microgrids," *Nonlinear Analysis: Hybrid Systems*, vol. 39, p. 100972, Feb. 2021.
- [40] B. Elibol, G. Poyrazoglu, B. C. Caliskan, H. Kaya, C. Armagan, H. E. Akinc, and A. Kaymaz, "Battery Integrated Off-grid DC Fast Charging: Optimised System Design Case for California," 2021 10th International Conference on Renewable Energy Research and Application (ICRERA), Sep. 2021.
- [41] M. A. Sörös and B. Hartmann, "Analysis of the Relation between State of Health and Self-Discharge of Li-Ion Batteries," *Acta Polytechnica Hungarica*, vol. 18, no. 10, pp. 225-244, 2021.